2007 IEEE International Conference on
Robotics and Automation
Roma, Italy, 10-14 April 2007

Piecewise-Linear Pattern Generator and Reflex System for Humanoid Robots

Riadh Zaier and Shinji Kanda
Autonomous System Laboratory
Fujitsu Laboratories Limited
Atsugi, Japan
zaier@labs.fujitsu.com *s.kanda@jp.fujitsu.com*

***Abstract*— Reflexes have been viewed as integrated motions with the centrally generated motors commands to produce adaptive movement. In this paper, a walking pattern generator for humanoid robots based on piecewise linear functions and inspired by passive walking is considered. To deal with lateral and frontal disturbances, sensory feedback is realized based on the inverse pendulum model. The reflex system that highly adapts and controls the movement of the humanoid robot, when a large disturbance occurs, is combined with the motion pattern generator and proposed in a unified form with regards to three types of sudden events. Experiments using Fujitsu's humanoid robot HOAP-3 demonstrate that a reflex movement is successfully integrated with the rhythmic motion when there are sudden changes in floor level, when obstacles suddenly appear, and in the presence of a large disturbance. The proposed reflex system therefore contributes toward the safe interaction of humanoid robots with the environment.**

Index Terms – Humanoid robot, Reflexes, Rhythmic motion, Motion generation, Piecewise-linear function, Linear oscillator.

I. INTRODUCTION

Motion control of humanoid robots has attracted considerable attention during the last decade. Much work has been focused on the dynamics of the robot using the zero moment point (ZMP) approach [1], [2]. Huang et al. [3] proposed a method for planning a walking pattern, where the reference trajectory is designed offline for given constraints on the foot and ground, and satisfying a particular ZMP constraints using third order spline functions. More recently, biologically inspired control strategies have been proposed to generate autonomously adaptable rhythmic movement. These are based on a neuronal network, termed a central pattern generator (CPG) [4-6], that is capable of generating a rhythmic pattern of motor activity in the absence of sensory input signals. Taga [5], [6] has demonstrated that bipedal locomotion can be realized as a global limit cycle generated through entrainment between a neural network consisting of a neural oscillator and the physical system.

On the other hand, toward a safe interaction of the humanoid robot with the environment, Morisawa et al. [7] presented a method to generate an emergency stop motion based on the evaluation on the ZMP and the center of gravity (COG). Okada et al. [8] presented a motion emergency system based on attractor design of the nonlinear dynamical system. Huang et al. [9] proposed a feedback sensory reflex, which consists of ZMP reflex, landing-phase reflex, and a body-posture reflex. Although the ZMP is controlled to strictly follow a desired path within a pre-defined ZMP stable region, the control does not allow the robot to move quickly. Moreover, in the presence of disturbances, the ZMP will have an arbitrary location that can be out of the stable region in spite of the stability of the robot's upper body.

In this paper, instead of using nonlinear dynamics models and solving complex equations, the control strategy is simply based on linear oscillators and few parameters that can be easily tuned. Moreover, the motivation is to provide a humanoid robot with reflexes to guarantee safe interaction with the environment. For this, the proposed method of motion generation also has the merit of facilitating the introduction of the reflex motion. To generate a walking motion, there are no constraints to satisfy on robot's foot or ZMP stability margin such as in [3], we simply use piecewise-linear functions and a first order low-pass filter generated by an original recurrent neural network (RNN) [10], where the "integrate and fire" neuron model [11] has been used. In our previous work [12] the method is straightforward with respect to three design parameters namely, the slope of the piecewise function, the time delay of the low pass-filter, and the rolling value defined by the static stability at the single support phase. The pitching motion of the robot, however, is roughly generated, then adjusted using a virtual spring-damper systems. To improve the robustness of the walk motion, a gyro sensor feedback loop is added to the overall control system.

As for the reflex system, instead of realizing each reflex separately [9], [12], it is realized in a unified fashion. For this, a simple recognizer based on Bayes rule is used to detect unexpected events. In this research framework, we 1) add normal feedback signals when a relatively small disturbance is detected by the gyro sensor; 2) change the walk parameters such as the gait, the stride, or the walk posture; 3) add an extra motion at some joints besides the motion generator outputs; 4) stop the walk motion in the case of large disturbance and generate a reflex based on the sensory data and an interpolation of four predefined postures. It should be noticed that the reflexes in 1) and 4) are decided according to the robot's upper body oscillation rather than the ZMP stability margin [9]. Moreover, since the leg during swing phase is made very compliant, there will be no tipping over when landing or colliding with an obstacle.

The rest of this paper is organized as follows. Section 2

describes the proposed motion pattern generator; Sections 3 presents the recognizer of unexpected events; Sections 4, 5, 6 and 7 present case studies for reflexes demonstrated in experiments using Fujitsu's humanoid robot HOAP-3 [13], [14], and Section 8 concludes the paper.

II. Motion Pattern Generation

A. Primitive Motion

Shaping an arbitrary motion pattern takes effort to think about the functions that fit the desired task with regards to given constraints. On the other hand, continuous piecewise linear functions have proved to be very powerful tools in modeling and analyzing nonlinear systems. For instance, to fit the real dynamics of the robot, the profile of the rolling motion of a humanoid robot can be approximated using (1).

$$\varepsilon_i \frac{da(t)}{dt} + a(t) = c(t)\,, \tag{1}$$

where $c(t)$ is the input signal described as a piecewise linear function in time t, $a(t)$ is the activation function. In fact, for small oscillations the passive behavior fits a sine-wave. But, in general, the trajectories for the biped joints are not sine functions with only one frequency component. For such situations, a combination of more primitive functions will be more interesting. The input signal $c(t)$ can be expressed as time series of N piecewise-linear functions $u_i(t)$:

$$c(t) = \sum_{i=1}^{N} c_i u_i(t - t_i)\,, \tag{2}$$

where $u_i(t) \in [0,1]$, $t_i \geq 0$ and c_i is a real number.

B. Rhythmic pattern generator for walking

B1. Rolling motion

The rhythmic motion is generated with regards to the rolling motion, which has a trapezoidal form, and smoothed using (1) as shown in Fig.1 (a). Notice that simple tuning of these parameters may lead to a good approximation solution of the inverse pendulum problem. To formulate the rolling motion pattern, let the rolling be a function with regards to the time delay ε, joint angular velocity ω, walking period T, and rolling amplitude A_r. Notice that A_r represents the static rolling that is required to maintain the center of gravity inside the supporting polygon.

$$\theta_r = f(\varepsilon, \omega, T, A_r)\,, \tag{3}$$

where $\theta_r(t)$ is the angular position to the rolling joints of the hip and ankle, and let $u(t_i, \omega_i) = \omega_i(t - t_i)$ with $0 \leq u(t_i, \omega_i) \leq 1$ According to Fig. 1 (b) the rolling can be expressed as

$$\varepsilon \frac{d\theta_r(t)}{dt} + \theta_r(t) = A_r(u(t_{r0}, 2\omega_r) - 2u(t_{r0} + (n + f_1)T, \omega_r) + 2u(t_{r0} + (n + f_2)T, \omega_r))\,, \tag{4}$$

where t_{r0} is the start time of the rolling motion, and n is number of walking steps. The f_1 and f_2 are the relative times with regards to the gait. By letting $p = t_{r1} - t_{r0} - 1/\omega_r$ be the time during which the robot stays at the maximum rolling, we can write $f_1 = (1/\omega_r + p)/T$ and $f_2 = 2f_1 + 1/(\omega_r T)$.

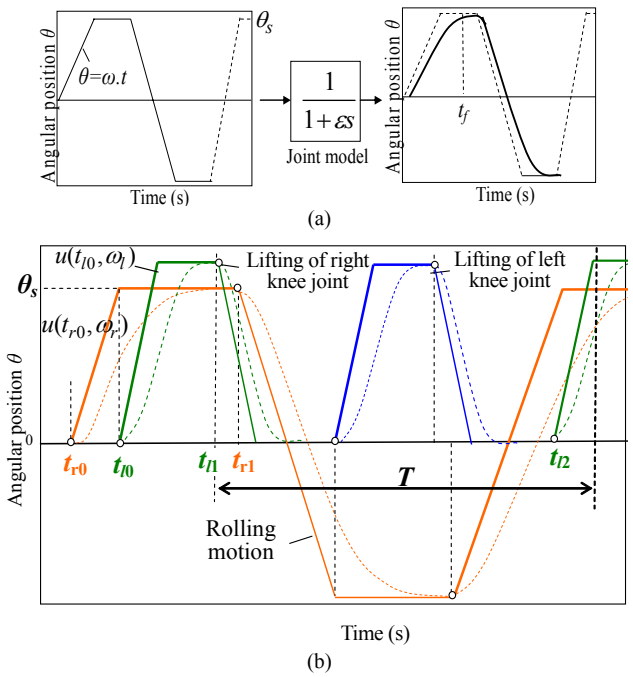

Fig. 1 Rolling motion pattern and design parameters.

B2. Swing motion

The swing motion is generated by the following equations as shown in Fig.1 (b).

$$\varepsilon \frac{d\theta_l(t)}{dt} + \theta_l(t) = A_l(u(t_{l0}, \omega_l) - u(t_{l1} + nT, \omega_l)) + u(t_{l2} + nT, \omega_l)) \tag{5}$$

$$\varepsilon \frac{d\theta_s(t)}{dt} + \theta_s(t) = A_s(u(t_{s1} + nT, \omega_s) - u(t_{s2} + nT, \omega_s))\,, \tag{6}$$

where θ_l is the lifting motion, θ_s is the angular position that generates the stride. A_l and A_s are the amplitude of lifting and stride length, respectively. The t_{l0} and t_{l2} are the start time of lifting motion. The t_{l1} represents the start time of landing phase and ω_l and ω_s are the joints' angular velocity generating the lifting motion and the stride, respectively.

On the other hand, the landing of each leg is accomplished with flat foot on a flat ground. Assuming that the thigh and shank of the robot have the same length, and with respect to the angles definition in [14], this condition can be satisfied using (5) and (6) as follows.

$$\begin{cases} \theta^p_{am}(t) = \theta_l(t) + \theta_s(t) \\ \theta_{km}(t) = -2\theta_l(t) \\ \theta^p_{hm}(t) = \theta_l(t) - \theta_s(t) \end{cases}, \tag{7}$$

where θ^p_{am}, θ_{km}, and θ^p_{hm} are the pitching motor commands to the ankle, the knee and the hip, respectively.

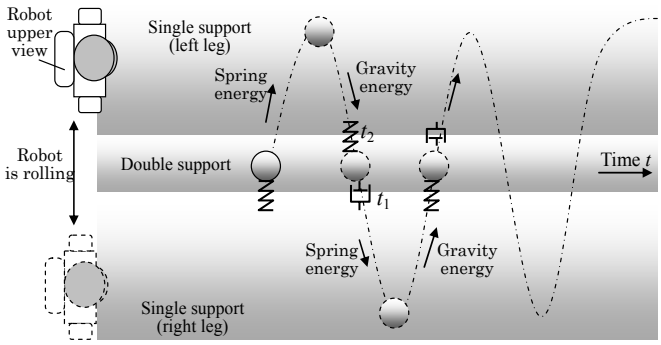

Fig. 2 Rolling motion with regards to time, inspired by passive walking. At t_1 the damper is used to land softly, while at t_2 the spring energy is used to lift.

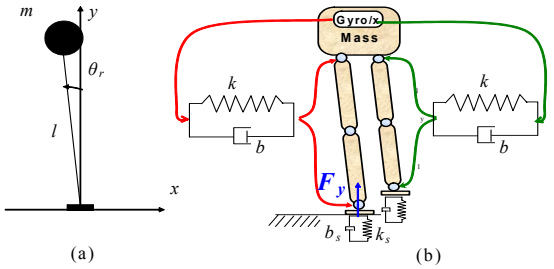

Fig. 3 Single support phase of humanoid robot.
(a)Inverse pendulum. (b) Control against lateral disturbances.

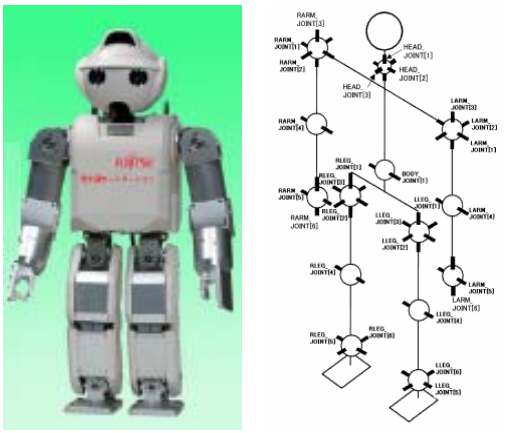

Fig. 4 HOAP-3 Standing pose and configuration.

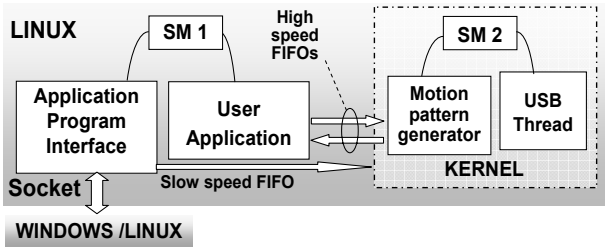

Fig. 5 Structure of the motion control system.

B3. Walking inspired by passive dynamics

Operating near a passive gait cycle is energetically efficient compared to other control strategies. The passive walking robot, which was originally pioneered by McGeer's [15], describes the gait of bipedal locomotion as a natural repetitive motion of a dynamical system or, in the language of nonlinear dynamics, a limit cycle. In this paper, although the passive dynamics idea is used, the oscillator is proposed as a piecewise-linear system. This type of control is much easier to analyze than control based directly on non-linear equations. Moreover, it provides much intuition about the system behavior.

Fig. 2 describes how the robot uses gravity for landing. Furthermore, a virtual damper-spring is added to the system such that the spring energy is pumped into the system allowing the lifting of the leg. The passive control idea in this research frame work is applied with regards to the rolling motion, which is realized by controlling the rolling amplitude such that the robot leg lands by gravity without relying on any ZMP stability constraint. Moreover, to minimize the force of the collision of the landing leg with the ground, instead of using impact model, besides (7), we control the damping factor b_s and the spring stiffness k_s of the virtual damper-spring system (8) such that the leg is very compliant at the swing phase, and gradually get stiffer till it reaches the maximum stiffness at the single support phase. Notice that the virtual spring-damper gets input from the force sensors located under each leg as shown in Fig. 3(b).

$$m\frac{d^2y_c(t)}{dt^2}+b_s\frac{dy_c(t)}{dt}+k_sy_c(t)=F_y, \qquad (8)$$

where $y_c(t)$ is the displacement of the mass m along the vertical axis, and F_y is the external force acting on the supporting leg. The angular positions to the motors' commands becomes

$$\begin{cases}\theta^p_{am}(t)=\theta_l(t)+\theta_s(t)+\theta_c(t)\\ \theta_{km}(t)=-2\theta_l(t)-2\theta_c(t)\\ \theta^p_{hm}(t)=\theta_l(t)-\theta_s(t)+\theta_c(t)\end{cases}, \qquad (9)$$

where $\theta_c(t)=\arcsin(y_c(t)/L)$ is the angular position induced by the virtual damper spring system in (8), and L is the length of the thigh.

B4. Stability robustness

In this section, the system's stability in the presence of lateral disturbance is considered. To deal with this, the dynamics of the inverse pendulum (Fig. 3a) with regards to the rolling motion is considered as follows.

$$\Gamma\frac{d^2\theta}{dt^2}-mgl\sin\theta=\tau, \qquad (10)$$

where g is the gravity constant, θ is the rolling angle, Γ is the moment of inertia of the robot upper body, and τ is the torque acting on the ankle of the supporting leg. To ease the control of the rolling motion, we use the linear approximation of the original nonlinear system around the equilibrium point, and (10) can be simplified to the following form:

$$\Gamma\frac{d^2\theta}{dt^2}-mgl\theta=\tau. \qquad (11)$$

For this linear plant model, two controllers are used (Fig.3 b) to maintain the upper body vertical to the ground, which get

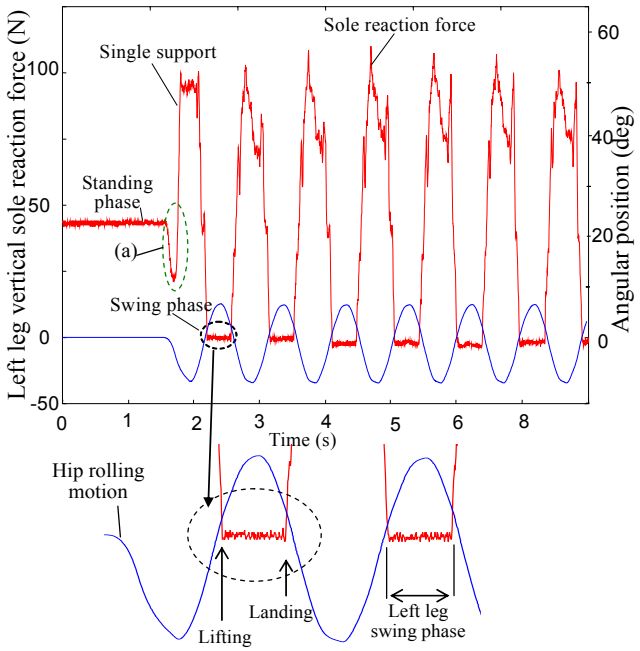

Fig. 6 Hip rolling joint output and sole reaction force acting on the left leg; (a) the robot uses spring energy when lifting. It uses gravity for landing.

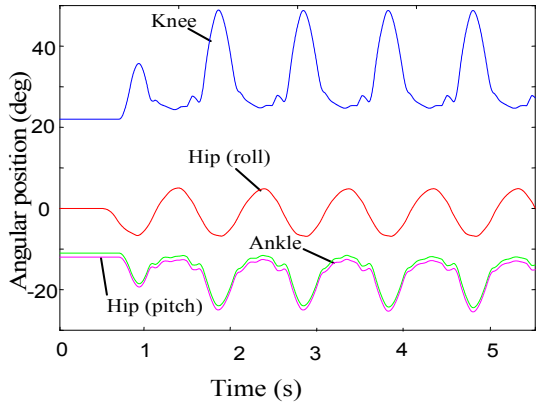

Fig. 7 Outputs of the joints of right leg.

input from the gyro sensor and feed back signals $\theta^r_{fb}(t)$ to the ankle and hip as

$$\theta^r_{am}(t) = -\theta^r_{hm}(t) = \theta_r(t) + \theta^r_{fb}(t) \qquad (12)$$

For further improvement of the walking performance, a simple ZMP feedback controller using directly the force sensors' inputs is added to the motion control system.

B5. Experiment

For the experiment, we used Fujitsu's humanoid HOAP-3 (Fig. 4), which has 28 joints, is 60cm tall, and weights 8.8 kg. The real-time control algorithms are implemented in real-time threads running in the RT-Linux kernel space as shown in Fig. 5. Kernel mode shared memory (SM) is constructed for the communication between real-time threads. The control period is 1 ms, and the RNN interface with the robot uses a real-time USB driver thread. Fig. 6 demonstrates how the robot uses gravity for landing and the spring energy for lifting. Fig.6 (a)

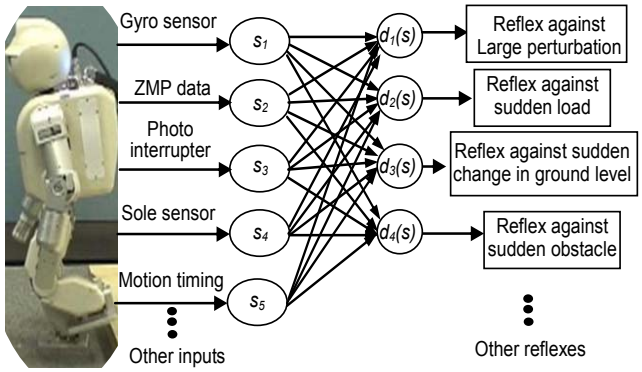

Fig. 8 General structure of the unexpected pattern recognizer, where s_i represents the normalized input signal and $d_i(s)$ is the discriminant function.

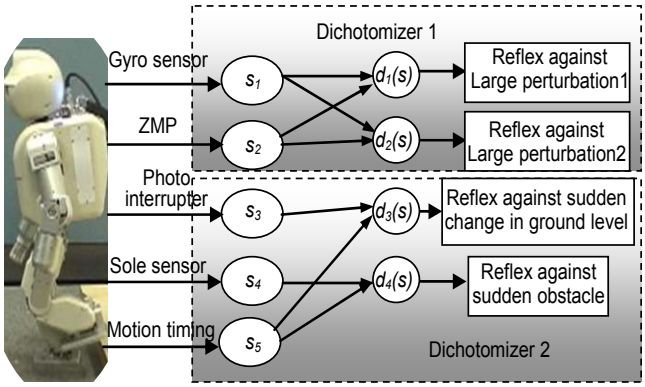

Fig. 9 Structure of the unexpected pattern recognizer after features extraction.

shows that the lifting phase starts when the angular position of the rolling joints is almost zero. In other words, the actuators of the hip and ankle rolling joints do not contribute in moving the ZMP to the supporting leg. These joints, therefore, can be considered as locked joints. Fig. 7 shows the rolling of the hip and the pitching motions of the knee, hip, and ankle. It also demonstrates how smooth the approximate solution using the proposed pattern generator with sensory feedback, where the profile of the rolling motion is very close to a sine function.

Remark: As detailed previously, the motion control method in this paper does not involve constraints on humanoid robot's foot or ZMP stability margin as in [3], it is based on the generation of a rough pitching motion adjusted and stabilized by sensory feedback. Moreover, the method allows motion pattern generation for fast walking.

III. Unexpected Event Recognizer

When the humanoid robot suffers a sudden deviation from its stable state, there will be a reflex action depending on the type of disturbances. For instance, consider that the robot is walking and encounters a sudden change in the ground level. This can be recognized when the robot does not touch the ground at the expected timing. For several types of undesired event, a recognizer will be necessary to decide the reflex action. When prior knowledge about the type of sudden event

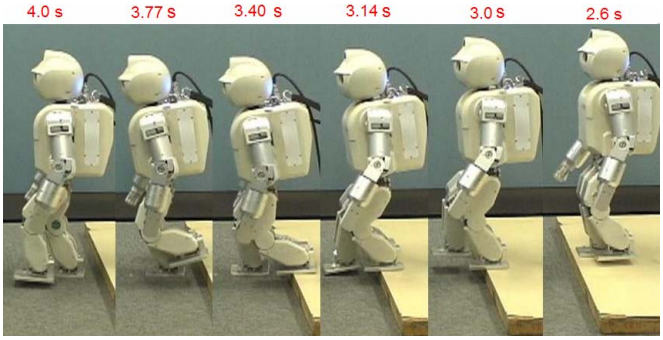

Fig. 10 HOAP-3 walking and encountering a sudden change in ground level.

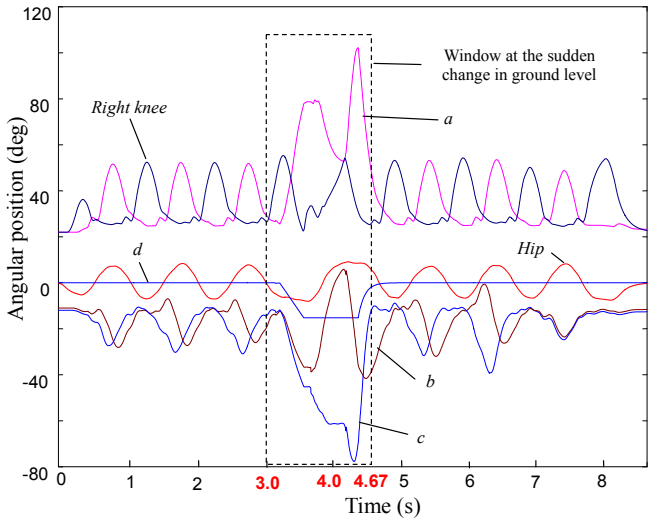

Fig. 11 Joints outputs at the sudden change in ground level. Pitching of the knee (*a*), ankle (*b*), and hip (*c*) joints of the left leg. (*d*): Extra motion added to the pitching joints of supporting leg.

is provided, and by defining a discriminant function $d_i(s)$ based on the Bayes rule, the general structure of the recognizer can be represented as shown in Fig. 8. In this research frame work, the recognizer is limited to four types of sudden events. To build up the recognizer, sensory data and motion related parameters are collected. When extracting the appropriate features required for each type of sudden event, we realized that the recognizer can be simplified into two dichotomizers (Fig. 9). The first dichotomizer consists of reflex actions against large disturbances. That is, when an input from the gyro sensor s_1 exceeds a given threshold, discriminant functions d_1 and d_2 will use that feature but the decision will depend on input's feature s_2. For instance, when the ZMP remains inside the support polygon, the disturbance is considered to be type one. If the ZMP leaves the support polygon, then a disturbance will be of type two. For example, pushing a robot as it is walking can be classified as a large disturbance of type one if the ZMP remains inside the supporting polygon, otherwise, it is of type two. As for the second dichotomizer, $d_3(s)$ activates the reflex action against a sudden change in ground level when the photo-interrupter that is attached to the front of the leg is enabled at landing time, while $d_4(s)$ activates the reflex against a sudden obstacle when the sole sensor of the swing leg touches an obstacle.

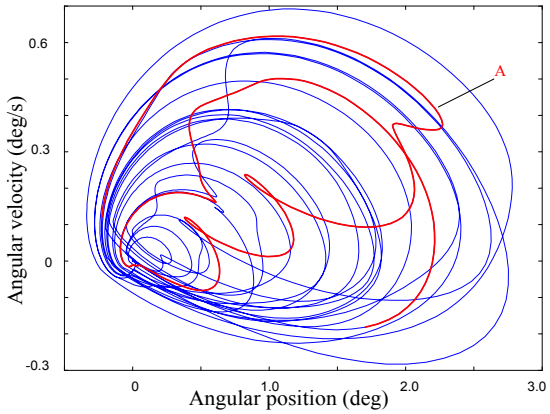

Fig. 12 Phase portrait for the upper body along the pitching direction.

In the following sections each reflex action will be detailed and demonstrated by experiment results.

IV. Reflex Against Sudden Change in Ground Level

A. Problem Description

In this section, we consider the case of reflex when the humanoid robot detects a sudden unknown change in the ground level. The reflex process is abstracted as follows:

- Detect the sudden change in the ground level.
- Add the necessary extra motion to maintain stability.
- Modify the gait using a touch sensor.
- Increase the stride to avoid collision with the ground.
- Use force sensor feedback to track the desired ZMP.

B. Detection of the ground level change and reflexes

The sudden change in ground level is detected using the recognizer in Fig. 9. That is, when the photo-interrupter, which is attached to the front of the robot foot, is enabled at the landing time of the leg, the appropriate reflex action will be triggered. We assume here that the change in ground elevation is unknown but within the hardware limit. The reflex action consists of increasing the stride so that the foot does not collide with the upper ground. On the other hand, the supporting leg will be contracted in height till the swing leg touches the lower surface. After landing, the walk parameters (gait and stride) will return to the previous ones. In this step, gyro feedback for both rolling and pitching is used (Fig. 3).

C. Experiment

Fig. 10 shows HOAP-3 walking on a surface with a sudden unknown change in level. The walking gait cycle is 0.5 s. The joints' outputs at the sudden change in ground level are shown in Fig. 11. The extra motion (*d*) is added to the supporting leg joints contracting the leg in height. The contraction is stopped when the swing leg touches the lower surface. The contraction phase of the supporting leg starts when the linear velocity of the upper body is almost zero. Moreover, the contraction speed is low enough to ensure that the contracting leg will not affect the stability of the robot. The walking cycle time is augmented by about 50% at the sudden change in ground level (Fig. 11). The motion of the supporting leg is modified accordingly. The phase portrait

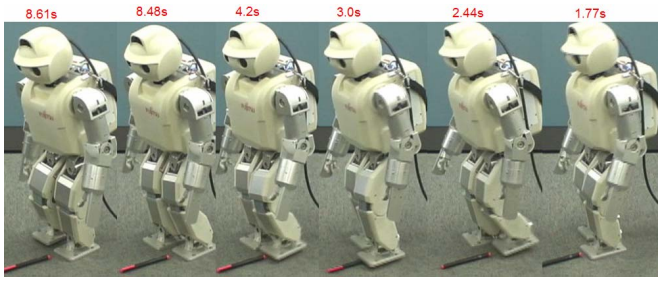

Fig. 13 Reflex against a sudden obstacle while walking.

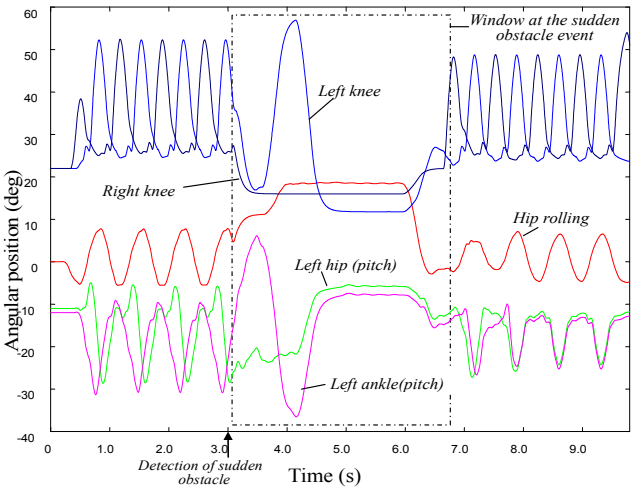

Fig. 14 Joints outputs when reflex against sudden obstacle is activated

of the angular velocity of the body and the angular position to the ankle and hip stabilizing the robot is shown in Fig. 12. The oscillation (*A*) occurs at the sudden change in ground level only, which is compensated afterwards.

V. Reflex Against Sudden Obstacle

A. Problem

In this section, we consider the case of reflex when the humanoid robot detects a sudden obstacle. The reflex process is abstracted as follows:

- Detect the sudden obstacle with a sole sensor.
- Stop the motion of the robot.
- Move the swing leg back to its previous position at the supporting phase.
- Resume the walking motion with negative stride, then stop or follow upper level control.
- Use force sensor feedback to track the desired ZMP.

B. Detection of a sudden obstacle

Using the proposed recognizer in Fig. 9, and as mentioned previously, this type of reflex is activated when a sudden obstacle touches the sole sensor of the leg in the swing phase. We assume here that the foot of the leg remains parallel to the ground during the swing motion, which is satisfied by (7).

C. Experiment

Fig. 13 shows the experiment results when HOAP-3 detects a sudden obstacle as it walks. The joints' outputs are

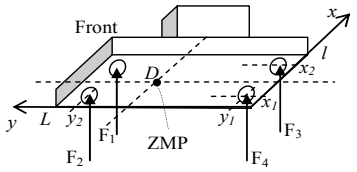

Fig. 15 Sole reaction forces on the foot and ZMP.

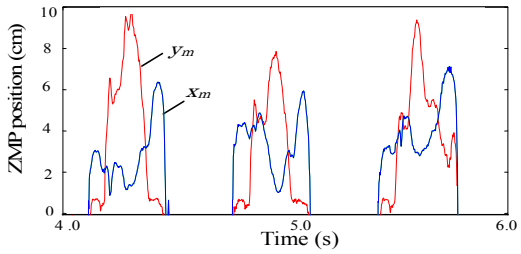

Fig. 16 Plot of the ZMP during stepping motion.

shown in Fig. 14. At 3.0 s, the sole sensor of the left leg touches the obstacle and the robot stops landing its leg and increases its rolling motion while keeping the gyro feedback controller active. The robot, then, retracts the left leg to its previous landing position. This is shown in Fig. 14 by the pitching motion of the hip, knee, and ankle within the time interval [3.0s, 4.8s]. The walking is resumed successfully at 6.8 s. Notice that the leg during swing motion is made very compliant as expressed in (8), where the stiffness is controlled during the gait. The stiffness of the leg at the middle of the supporting phase is the highest, while it is the lowest during the swing phase.

VI. Reflex Against Large Disturbance

A. Problem

The humanoid robot is pushed as it walks, causing a large disturbance in its movement that could not be compensated by a normal feedback controller. In this case, the recognizer in Fig.9 will activate the reflex movement against large disturbances type two. The direction of the pushing force is calculated using the sole reaction force. Four postures around the walking motion are defined, which we called learned postures. When a large perturbation occurs, the robot will stop walking and shift its posture to one of learned postures selected according to the sole reaction force. The gyro feedback controller will be active around the final pose the humanoid robot has shifted to.

B. Reflex movement.

Instead of writing equilibrium equations of forces and moments acting on the robot body, we limit the analysis simply by the use of the sole reaction forces measured by sole sensors as shown in Fig.15. The idea is based on the evaluation of the shift in the ZMP position, using foot force sensor data. Let $D(x_m\ y_m)$ be the position of the ZMP where the reaction torques are null. Moreover, the ZMP during normal condition (No large disturbance is present) will be calculated and recorded at each single support phase. The four postures to which the robot can shift when it stops walking involve moving the leg to the front, back, right, or left, according to the ZMP position. Then, a feedback

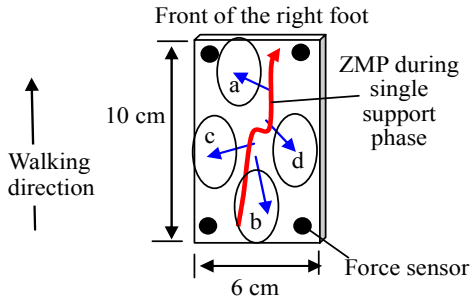

Fig. 17 ZMP trajectory at the single support phase and zones (a, b, c, and d) to which the ZMP will shift when disturbance occurs.

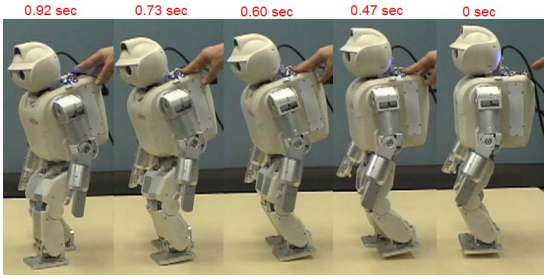

Case 1: The ZMP has shifted to zone (a) in Fig. 17.

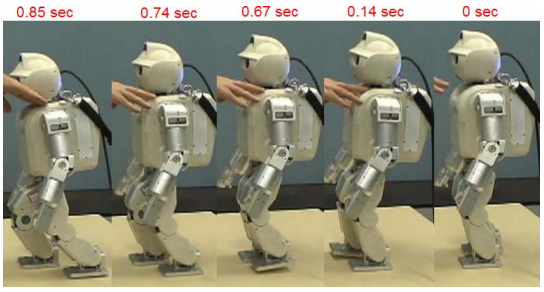

Case 2: The ZMP has shifted to zone (b) in Fig. 17.

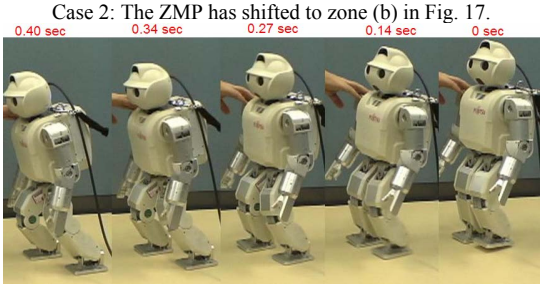

Case 3: The ZMP has shifted between zones (b) and (d) in Fig.17.

Fig. 18 Reflex against large disturbance.

controller will be active at the final posture controlling the robot waist and legs joints.

C. Experiment

Fig. 16 shows the ZMP location during walking with a zero stride and in the absence of a disturbance, which is calculated using (13) and (14). The ZMP during normal walking can be represented as shown in Fig.17. Accordingly, as previously mentioned, we define four zones where, if the ZMP is shifted to in the presence of large disturbance type two (Fig.9), the robot will stop walking and modify its posture.

$$y_m = \left(y_1(F_3 + F_4) + y_2(F_1 + F_2)\right) / \sum_{i=1}^{4} F_i \,. \qquad (13)$$

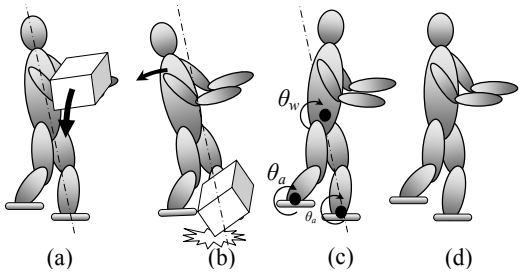

Fig. 19 Proposed control policy at a sudden change in load; (a) The robot is carrying a box, (b) The box is fallen down, (c) generation of reflex motion in the waist and ankle joints, (d) ZMP and Gyro feedback control.

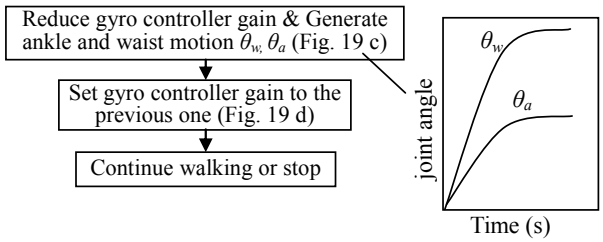

Fig. 20 Flowchart of reflex at sudden change in load.

$$x_m = \left(x_1(F_2 + F_4) + x_2(F_1 + F_3)\right) / \sum_{i=1}^{4} F_i \,. \qquad (14).$$

When the ZMP shifts between these four zones, linear interpolation will be considered between the defined postures as demonstrated in Fig. 18 (case 3), where the ZMP is between zone (b) and zone (d), and the left leg is moved back to the left side.

VII. Reflex Against Sudden Change in Load

A. Problem

In this section, we consider the reflex when the humanoid robot detects a sudden change in load as it walks, which is considered as a large disturbance of type one (Fig. 9). The proposed reflex policy is shown in Figs. 19 and Fig. 20. The reflex motions θ_w and θ_a will be generated simultaneously at the ankles and waist joints, respectively (Fig. 19 c). The amplitudes of these angles are set according to the deviation angle of the upper body. During this phase only, the gain of the gyro feedback controller, which works against oscillation of the robot's upper body, is reduced by more than half. After this phase, the gain of the gyro feedback controller is set to its previous value (Fig 19 d).

B. Experiment

Fig. 21 shows HOAP-3 carrying a relatively heavy box (500 g). As it walked, the box was taken away and the robot could walk stably and compensate for the change by adjusting its walking posture at the ankle and waist joints according to the algorithm in Fig. 20. The positions of the ankles and their change during walking are shown in Fig. 22. The reflex motion is generated within the time interval [6.0s, 7.0s]. It should be noticed here that the reflex is triggered by the gyro sensor when its value exceed a given threshold, while the reflex motion is selected according to the recorded ZMP at the disturbance detection time.

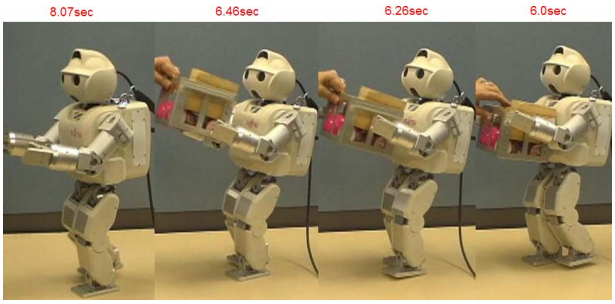

Fig. 21 Reflex against sudden change in load while walking.

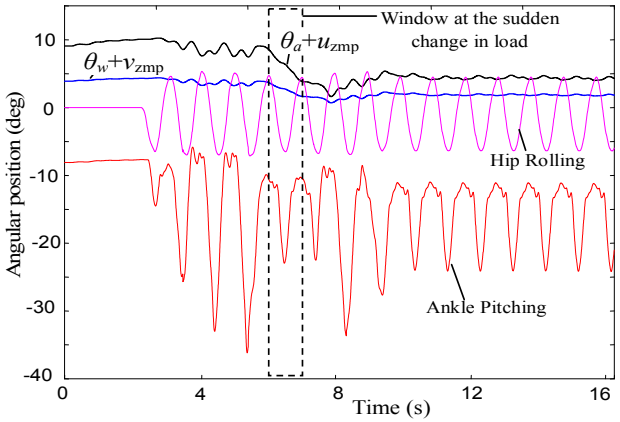

Fig. 22 Joints outputs at the sudden change in load. As shown in Fig. 20, θ_a, and θ_w are the angles added to the ankle and waist joints, respectively. u_{zmp}, and v_{zmp} are the ZMP feedback controls to the ankles and waist joints.

VIII. Conclusion

This paper presented a walking pattern generator with a reflex system for humanoid robots. The reflex system was combined with the motion pattern generator to improve the robustness against lateral and frontal disturbances. The walking motion becomes adaptive so that a robot would be able to walk on floor, carpet, and slope. The reflexes that highly adapt and control the movement of the humanoid in the presence of large disturbance were considered in a unified form.

In order to demonstrate the effectiveness of the proposed system, we used Fujitsu's humanoid robot HOAP-3. It was shown that a reflex movement was successfully enabled and integrated with the rhythmic motion in the cases of a sudden change in the floor level and a sudden obstacle, and in the presence of a large disturbance. The proposed reflex system therefore has contributed toward the safe interaction of humanoid robots with the environment.

As a future work, we will extend the result to the interaction between the upper and lower body of the humanoid robots. Moreover, we will consider a systematic features extraction method suitable for the proposed recognizer.

Acknowledgment

The authors would like to thank Dr. Hada Yoshiro of Fujitsu Laboratories Ltd., for his useful comments.

References

[1] H. Miura, I. Shimoyama, "Dynamic walk of a biped", *The International Journal of Robotics Research*, 1984, vol. 3 no. 2, pp.60-74.

[2] S. Kajita, O. Matsumoto, "Real-time 3D walking pattern generation for a biped robot with telescopic legs", *Proceeding of the 2001 IEEE International Conference on Robotics & Automation*, 2001, pp.2299-2306.

[3] Q. Huang, K. Yokoi, S. Kajita, K. Kaneko, N. Koyachi, H. Arai, and K. Tanie, "Planning walking patterns for a biped robot," in *IEEE Trans. Robotics and Automation*, vol. 17, no. 3, pp. 280–289, Jun. 2001.

[4] S. Grillner, "Neurobiological bases of rhythmic motor acts in vertebrates", *Science*, 1985, no. 228, pp143-149.

[5] G. Taga, "A model of the neuro-musculo-skeletal system for human locomotion, I. Emergence of basic gait", *Boil. Cybern*, 1995, no.73, pp.97-111

[6] G. Taga, Y. Yamaguchi, and H. Shimizu, "Self organized control of bipedal locomotion by neural oscillators in unpredictable environment", *Biological Cybernetics*, 1991, vol. 65, pp.147-159.

[7] M. Morisawa, S. Kajita, K. Harada, and K. Fujiwara, "Emergency Stop Algorithm for Walking Humanoid Robots," *IEEE/RSJ International Conference on Intelligent Robots and Systems*, 2005, pp. 2109- 2115.

[8] M. Okada, K. Osato, and Y. Nakamura, "Motion Emergency of Humanoid Robots by an Attractor Design of a Nonlinear Dynamics," *IEEE International Conference on Robotics and Automation*, 2005, pp. 18- 23

[9] Q. Huang, Y. Nakamura, "Sensory Reflex Control for Humanoid Walking" in *IEEE Trans. Robotics and Automation*, vol. 21, no.5, pp. 977-984, Oct. 2005.

[10] R. Zaier, and F. Nagashima, "Motion Generation of Humanoid Robot based on Polynomials Generated by Recurrent Neural Network", *Proceedings of the First Asia International Symposium on Mechatronics*, 2004, p.659-664

[11] W. Gerstner, "Time structure of the activity in neural network models", *Phys. Rev*, 1995, E. 51, pp.738-758.

[12] R. Zaier, and F. Nagashima, "Motion Pattern Generator and Reflex System for Humanoid Robots", *Proceeding of IEEE/RSJ International Conference on Intelligent Robots and Systems,* 2006.

[13] Y. Murase, Y. Yasukawa, K. Sakai, M. Ueki, "Design of Compact Humanoid Robot as a Platform", *19th Annual Conference of the Robotics Society of Japan*, 2001, pp.789-790

[14] HOAP-3, Fujitsu Automation Ltd. Available: http://www.automation.fujitsu.com/group/fja/services/hoap/

[15] T. McGeer, "Passive dynamic walking", *International Journal of Robotics Research,* 1990. 9(2):62–82.